

A rebinning technique for 3D reconstruction of Compton camera data

Junqiang Li¹, John D. Valentine¹, John N. Aarsvold², Murat Khamzin¹,
¹Nuclear and Radiological Engineering Program, Georgia Institute of Technology
²Department of Radiology, Emory University

ABSTRACT: A newly developed 3D image reconstruction technique for Compton camera data is described in this paper. For Compton cameras, the energies and positions of gamma-ray interactions in at least two detectors from a single incident photon are recorded using coincidence techniques. Based on this information, the Compton scattering formula establishes a cone surface from which the incident photon must have originated. Through an extension of the previously developed rebinning technique, instead of tracing the entire cone surface into the image space, a number of lines on the cone surface are sampled. All the lines start from the apex of the cone and are evenly distributed over the cone surface. The number of lines on each cone is determined by the desired spatial resolution. Each line is then projected to a perpendicular imaginary detector plane. The 2D Fourier transform of the line-projection data on this plane is shown to be one rotated plane of the 3D Fourier transform of the source distribution in the frequency domain. By projecting all of the sampled lines, performing Fourier transforms on all of the projected data, and summing up all the transformed data in the frequency domain, the 3D Fourier transform of the source distribution can be obtained. Interpolation and geometry normalization of data points in the 3D frequency domain will subsequently be applied. An image can then be reconstructed by a 3D inverse Fourier transform. The development of this technique will be discussed in detail.

I. INTRODUCTION

For a Compton scatter camera as illustrated in Figure 1 in which it is assumed that one emitted gamma ray Compton scatters in the primary detector then undergoes a photoelectric absorption in a secondary detector (this interaction sequence is defined as a preferred event), a cone surface can be established to determine the possible locations from where the incident photon was emitted [1-3]. The location and orientation of the cone surfaces are random in space and depend on where the two interactions occur in these two detectors, as well as the energies deposited. Thus image reconstruction is a difficult task. One potential 3D image reconstruction technique is the conventional Fourier deconvolution, which is based on projecting cone surfaces into the image space to establish a data matrix and then deconvolution of the projected data matrix with the point spread function that was previously determined for the image system [4]. In this study, a rebinning technique is being developed for the 3D image reconstruction of Compton camera data.

II. METHODOLOGY

Prior to describing the rebinning method for image reconstruction for Compton cameras, some aspects of rebinning need to be discussed. As illustrated in Figure 2, $f(x,y,z)$ is a function in 3D space and P is an arbitrary plane that crosses the origin O. A rotated coordinate system (O,X',Y',Z') is established such that the $X'-Y'$ plane is plane P. The relationship between the rotated coordinates and the global coordinates is simply a rotation operator R_p . Function $f(x,y,z)$ in the rotated coordinates will be:

$$f(x', y', z') = R_p [f(x, y, z)] \quad (1)$$

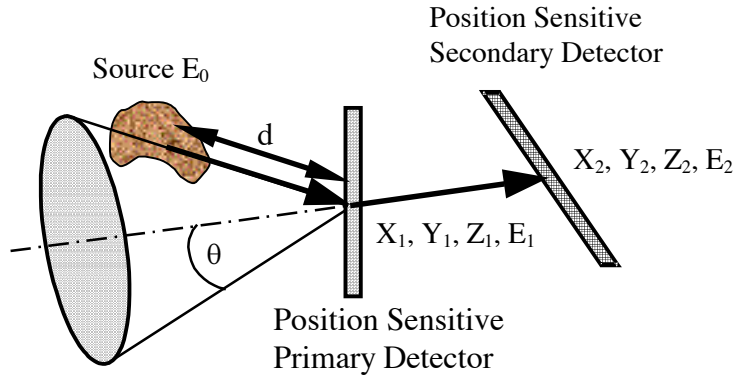


Figure 1. Principle of Compton scatter camera. E_1 and E_2 correspond to the energy deposited in the primary and secondary detectors, respectively.

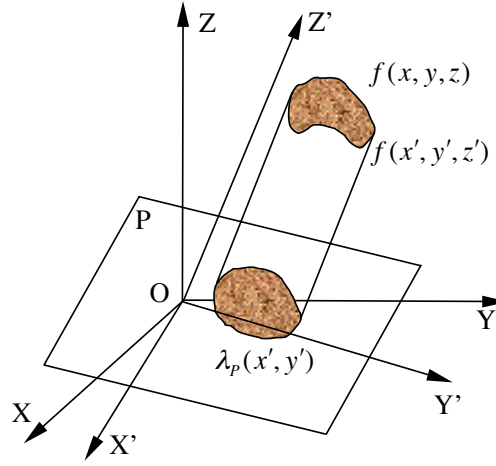


Figure 2. Projection of a 3D function $f(x', y', z')$ (in rotated coordinates) onto a plane P.

When $f(x, y, z)$ is perpendicularly projected onto P, it is projected along the Z' axis in the rotated coordinates. We denote this projection as $\lambda_p(x', y')$ in the rotated coordinate system:

$$\lambda_p(x', y') = \int_{-\infty}^{\infty} f(x', y', z') dz' \quad (2)$$

By taking the Fourier transform of $\lambda_p(x', y')$ on x' and y' , we get

$$\begin{aligned} \Lambda_p(u', v') &= F_2[\lambda_p(x', y')] = \int_{-\infty}^{\infty} dx' \int_{-\infty}^{\infty} \lambda_p(x', y') e^{-2j\pi(u'x' + v'y')} dy' \\ &= \int_{-\infty}^{\infty} dx' \int_{-\infty}^{\infty} dy' \int_{-\infty}^{\infty} f(x', y', z') e^{-2j\pi(u'x' + v'y')} dz', \end{aligned} \quad (3)$$

where the F_n operator is the Fourier transform operator of dimension n and u' and v' are the frequency components corresponding to x' and y' , respectively.

The 3D Fourier transform of $f(x', y', z')$ in the rotated coordinate system gives

$$F'(u', v', w') = F_3[f(x', y', z')] = \int_{-\infty}^{\infty} dx' \int_{-\infty}^{\infty} dy' \int_{-\infty}^{\infty} f(x', y', z') e^{-2j\pi(u'x' + v'y' + w'z')} dz'. \quad (4)$$

Comparison of equations (3) and (4) yields

$$\Lambda_p(u', v') = F'(u', v', w')|_{w'=0}. \quad (5)$$

The physical meaning for equation (5) can be stated as: the 2D Fourier transform of line-projection of a 3D function onto a plane is a directly rotated plane $(u', v', 0)$ through the 3D transform of the original function in the frequency domain. The rotated plane in frequency domain has the same orientation as the plane to which the function is projected. This can be seen as an extension of the central slice theorem of the Radon transform from 2D to 3D, although it is different from the 3D Radon transform [5-7].

The quickest route to calculate $f(x, y, z)$ with the knowledge of $\lambda_p(x', y')$ is through equation (5). If a complete set of projections are available, i.e. $\lambda_p(x', y')$ are known in every plane that crosses the origin, the Fourier transform of all projections will give the complete Fourier transform of the original 3D function. So $f(x, y, z)$ can be obtained as

$$f(x, y, z) = F_3^{-1}[F(u, v, w)] = \int_{-\infty}^{\infty} du \int_{-\infty}^{\infty} dv \int_{-\infty}^{\infty} \sum R_p^{-1}[\Lambda_p(u', v')] e^{2j\pi(ux + vy + wz)} dw, \quad (6)$$

where R_p^{-1} is the rotation operator transforming Λ_p from the rotated coordinates into the original coordinates in the frequency domain. Σ sums up all of the projections to establish the complete 3D Fourier transform of the original function.

III. REBINNING COMPTON CAMERA DATA

For the Compton camera, instead of tracing the entire cone surface into the source space to reconstruct an image, we propose to sample lines on the cone surface. All lines originate from the vertex of the cone surface and are evenly distributed over the cone surface. Consequently, we have two options for sampling $\lambda_A(x',y')$: 1) predefined planes and 2) arbitrary planes.

a) Predefined Planes

A series of planes each of which covers an equivalent solid angle and covers half of the sphere (i.e., a total solid angle of 2π is thus subtended) are predefined. Each line is projected onto one and only one plane to which this line is closest to being perpendicular. All of the planes that have projections from this sampled cone will mark the projected spot with a weighting factor such that when summing up all the points projected by the lines from one cone, the total weight is 1. In this manner, each cone represents only one valid event and shall contribute equally to the image.

After all of the cones have been rebinned, the 2D Fourier transform is performed on each of the predefined planes to get its frequency components. Each Fourier transform undergoes a rotation operation, according to the orientation of the plane, into the same universal coordinates. Summation of all of the rotated data, interpolation of data points where data are missing, as well as geometry normalization operations will then be employed. By performing 3D inverse Fourier transform on the summation of all the data, the original 3D function can be constructed.

b) Arbitrary Planes

An alternative means of calculating $\lambda_A(x',y')$ can be approached as follows. Each line on the cone surface can be treated as the norm to a plane, and therefore can define a plane that passes through the origin of coordinates. Since this line serves as the norm to the projection plane, the projection will be exact, no approximation is introduced as it was in a). Theoretically there will be the same total number of planes as the total number of lines, and each plane will only have one projection point. Since the Fourier transform and rotation are both linear operations, one can perform either the summation or Fourier transform in equation (4).

The second approach is still under development. The computational load seems to be very large for this method, since there will be one 2D Fourier transform for each sampled line. However, while all the plane sizes are the same, even though there might be only one point on this plane, there are only limited combinations of how this point is distributed over this plane. Therefore a table can be constructed *a priori* for the Fourier transform of every possible projection. By looking up the corresponding Fourier transform in the table, this time-consuming step may be executed relatively quickly.

III. PRELIMINARY RESULTS

For the rebinning strategy a) in the previous section, if the planes used here are a series of planes rotating along one single axis, and each plane only covers a small portion of solid angle, the image reconstruction is similar to standard SPECT. In this case, the filtered backprojection algorithm can be directly applied to the projection data to reconstruct the image. Figure 3 is an illustration of this case. 5 point sources are simulated using MCNP with 1.6 million preferred events.

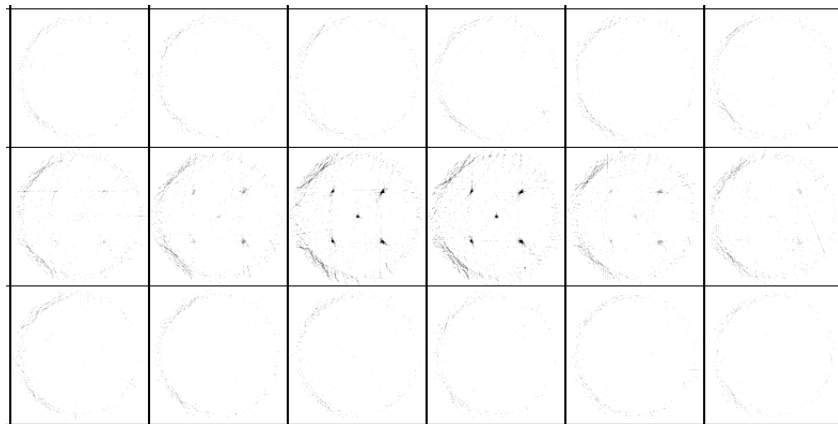


Figure 3. Reconstructed image with 5 point sources with equal activity. Only 18 out of 128 slices are shown here. 360 planes are used for projection, and they all rotate along the same axis with each one covering 0.5-degree angle in each direction.

With 360 planes rotating along the Z-axis and each covering an equal solid angle, 0.5 degrees azimuthally and 0.5 degrees in z direction, the filtered backprojection algorithm is adopted. No noise has been added to the simulation. Each slice covers a 22 cm \times 22 cm area and is divided into 128 \times 128 pixels. Distance between slices is the same as the space between pixels within one slice. Though only a very small portion of solid has been taken into account ($\sim 0.4\%$) for 1.6 million cones (i.e., only a small amount of data is used), the constructed image shows clearly the 5 point sources. Notice there are some artifacts around the edge of the image space. This kind of artifact is probably due to the fact that the lines are much denser at the vertex area, and it is possible to filter out this artifact by introducing certain types of filters during the reconstruction.

IV. SUMMARY

A rebinning technique for Compton camera image reconstruction is proposed and under development. Preliminary results show that this is a promising technique for fully 3D image reconstruction of Compton camera data. The full manuscript will provide a detailed discussion of this technique. The discussion will cover the derivation of the transform, analysis of the inverse transform, properties of this kind of transform in space domain as well as in frequency domain, and discussion on reconstructed images.

V. REFERENCES:

- [1] M. Singh, "An electronically collimated gamma camera for single-photon emission computed tomography. Part I: Theoretical considerations and design criteria," *Med. Phys.*, vol. 10, No. 4, pp. 421-427, 1983.
- [2] M. Singh and D. Doria, "An electronically collimated gamma camera for single photon emission computed tomography. Part II: Image reconstruction and preliminary experimental measurements," *Med. Phys.*, vol. 10, No. 4, pp. 428-435, 1983.
- [3] R. C. Rohe and J. D. Valentine, "An energy subtraction Compton scatter camera design for *in vivo* medical imaging of radio-pharmaceuticals," *IEEE Trans. Nucl. Sci.* vol. 43, No. 6, 1996.
- [4] P.E. Kinahan, J. G. Rogers, "Analytic 3D image reconstruction using all detected events", *IEEE Trans. Nucl. Sci.* vol. 36, No. 1, pp. 964- 968, 1989. J. G. Golsher, Fully three-dimensional positron emission tomography , *Phys. Med. Biol.*, vol. 25, No. 1, pp. 103-115, 1980.
- [5] S. R. Deans, *The Radon transform and some of its applications*, John Wiley & Sons, Inc. 1983.
- [6] H. H. Barrett, The Radon transform and its applications , *E. Wolf, Progress in Optics XXI*, Elsevier Science Publishers, pp. 219-286, 1984.
- [7] M. Defrise, A factorization method for the 3D x-ray transform , *Inverse Problems*, vol. 11, pp. 983-994, 1995.